Accepted Manuscript

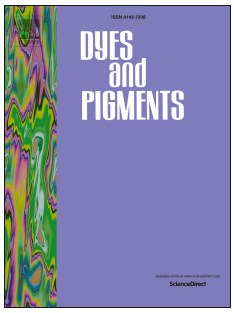

High contrast mechanofluorochromic behavior of new tetraphenylethene-based Schiff base derivatives

Ting Sun, Dandan Cheng, Yongshuai chai, Jian Gong, Mengyu Sun, Feng Zhao

PII: S0143-7208(19)30973-8

DOI: https://doi.org/10.1016/j.dyepig.2019.107619

Article Number: 107619

Reference: DYPI 107619

To appear in: *Dyes and Pigments*

Received Date: 6 May 2019

Revised Date: 28 May 2019

Accepted Date: 3 June 2019

Please cite this article as: Sun T, Cheng D, Yongshuai chai , Gong J, Sun M, Zhao F, High contrast mechanofluorochromic behavior of new tetraphenylethene-based Schiff base derivatives, *Dyes and Pigments* (2019), doi: https://doi.org/10.1016/j.dyepig.2019.107619.

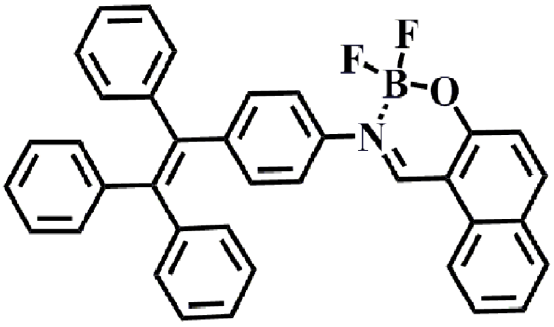

TPE-NDB

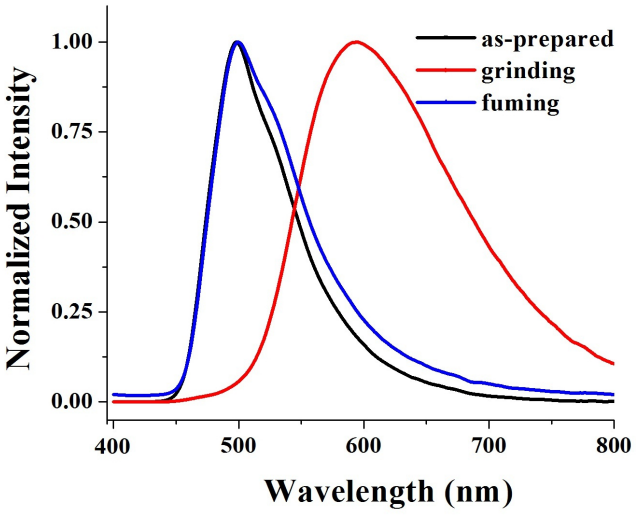

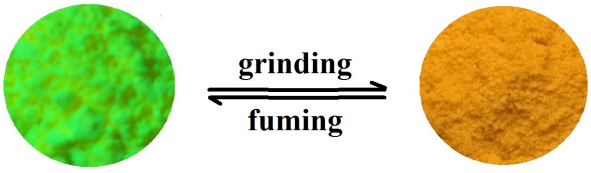

High Contrast Mechanofluorochromic Behavior of New Tetraphenylethene-based Schiff Base Derivatives

Ting Sun ,[a] Dandan Cheng,[b] Yongshuai chai,[c] Jian Gong,[a] Mengyu Sun,[a] Feng Zhao,[a, d, *]

[a] *College of Chemistry and Chemical Engineering, Anyang Normal University, Anyang 455000, P. R. China*

[b] *School of Life Science Wuchang University of Technology, No.16, Jiangxia Avenue, Wuchang, Wuhan 430223, P.R.China*

[C] *Interdisciplinary Research Center on Biology and Chemistry, Shanghai Institute of Organic Chemistry, Chinese Academy of Sciences,Shanghai 200032, P.R. China*

[d] *Henan Province Key Laboratory of New Opto-Electronic Functional Materials, Anyang 455000, P. R. China*

* Corresponding author. E-mail addresses: zhaofeng@aynu.edu.cn

Abstract

New tetraphenylethene-based Schiff base ligand (**TPE-ND**) and its corresponding boronated complex (**TPE-NDB**) with aggregation-induced emission were designed and synthesized. Results showed that the inhibited C=N isomerization by N, O-chelated BF_2 caused the significant intramolecular charge transfer features, and more dramatic solvatochromism. In particular, the solid sample of **TPE-NDB** exhibited an obvious mechanofluorochromic behavior. Upon grinding with a spatula, the as-prepared powder sample illustrated a remarkable red shift of 97 nm, with considerable color contrast from bright green (498 nm) to orange (595 nm). Its fluorescence color can be reversibly switched by repeating the grinding-fuming process. The mechanochromism is attributed to the phase transformation between amorphous and crystalline states. The practical application indicated that **TPE-NDB** has excellent mechanofluorochromic properties, and it can be utilized as optical recording materials.

Keywords: Tetraphenylethene-based Schiff base, boron complex, mechanofluorochromism, intramolecular charge transfer, aggregation-induced emission.

1. Introduction

Luminescent organic dyes have attracted much attention due to their potential for sensors, memory storage, organic light-emitting devices, and data security protection [1-4]. To date, design and creation of efficient luminescent dyes in the solid and aggregate states is still a hot research topic. A formidable challenge to this development is the notorious aggregation-caused quenching (ACQ) effect, namely, the emission of a conventional luminophore is usually weakly emissive or completely quenched upon aggregation in the solid state because of the formation of excimers and exciplexes [5]. Fortunately, in 2001, Tang's group developed a series of propeller-shaped silole compounds showing aggregation-induced emission (AIE) effect, which is exactly opposite to the troublesome ACQ phenomenon, and thus could overcome fluorescence quenching in aggregation [6]. Since then, numerous compounds with AIE properties have been explored, including tetraphenylethenes [7], fulvenes [8], 9,10-divinylanthracene derivatives [9], pyran derivatives [10], conjugated polymers [11] and others. In 2010, Park et al. reported the cyano-distyrylbenzene derivative with stimuli-responsive and AIEE properties, which has opened a new avenue of mechanofluorochromic (MFC) compounds. Then a number of both MFC and AIE dyes were synthesized by Tang, Chi, Yang and their co-workers [12-15]. In general, AIE-active compounds possess the strongly twisted skeleton bearing rotatable aryl units, which can afford loose packing patterns in the crystal states, could be easily destroyed under mechanical stimuli and cause the emitting color change. Currently, extended π-conjugated molecules with a D–A structure was very significant for the organic dyes to show MFC characteristics [16] and some D–A typed molecules always contribute to the realization of fluorescence change under mechanical force [17]. Tetraphenylethene (TPE) is a typical AIE unit,

which takes a nonplanar configuration and has electron donating characteristics. It to be a useful building block for the construction of D–A type dyes [12c, 13c, 18].

Despite a variety of AIE systems possessing reversible MFC features have been developed, most of the MFC dyes so far exhibit spectral shifts within tens of nanometers upon simple mechanical stimuli [18a, 19]. Reports of the dyes with very large MFC shifts (>90 nm) and obvious color contrast are still rare. The prominent color contrast before and after the application of mechanical stimulus are great important for the effective application of MFC materials. Moreover, these dyes are often prepared through complicated synthetic routes. It is highly demand to exploit high contrast MFC dyes using facile synthetic procedures. Schiff bases have the advantages of a rather facile synthesis with high yield and flexible structure modification. They have been explored extensively as catalysts [20], ions sensors [21], and pharmacological components [22]. However, the exploration of their MFC potential is still in the early stages [23].

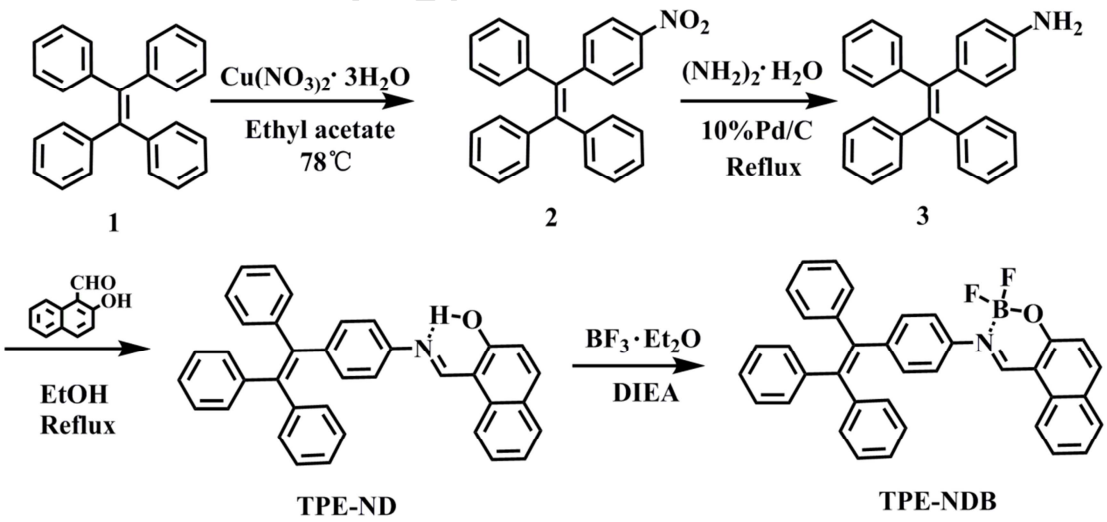

Scheme 1. Synthetic routes of **TPE-ND** and **TPE-NDB**.

In this perspective, we focus on the combination of tetraphenylethene (TPE) unit with conventional Schiff base functional segment to develop new MFC dyes with D-A structure. We synthesized the tetraphenylethene-based Schiff base ligand (**TPE-ND**) and its corresponding boronated complex (**TPE-NDB**), and their synthetic routes are shown in Scheme 1. AIE and MFC characteristics of the two fluorescent dyes were systematically investigated, and the results indicated that the ligand **TPE-ND** demonstrated the intramolecular charge transfer (ICT) nature and AIE property, whereas boronated complex **TPE-NDB** exhibited strong ICT feature, and obvious AIE and MFC characteristics. More importantly, MFC behaviors of **TPE-NDB** displayed a large spectral shift of 97 nm before and after mechanical stimuli. The remarkable MFC characteristics are desirable owing to their practical applications in mechano-sensors, memory devices, and forensic science [24-26].

2. Experimental

2.1. Materials and instrumentation

All reagents and solvents were purchased commercially (AR grade) and used without further purification unless otherwise noted. Tetrahydrofuran (THF) and toluene were distilled from sodium and benzophenone ketyl in a nitrogen atmosphere. Dichloromethane (DCM) was distilled from calcium hydride. The THF/H_2O mixtures with different water fractions were prepared by slowly adding distilled water into the THF solution of samples under ultrasound at room temperature. ^{1}H NMR and ^{13}C NMR spectra were collected on a Bruker–400 MHz spectrometer with TMS as an internal standard. Mass spectra were measured on a Shimadzu MALDI-TOF MS spectrometer. UV-vis spectra were recorded on Shimadzu UV-2550 spectrophotometer. Emission spectra were performed by a HITACHI fluorescence spectrometer (F-4600). The absolute fluorescence quantum yields and fluorescence

lifetime were measured on an Edinburgh FLS980 steady state spectrometer using an integrating sphere, and the lifetimes were calculated with the F900 Edinburgh instruments software. Crystal data of compound was selected on a Bruker D8 Focus Powder X-ray diffraction diffractometer. The geometry of the sample molecule was fully optimized using density functional theory (DFT) at the B3LYP/6-31G* level, employing the Gaussian 09W suit of programs. Dynamic light scattering (DLS) measurements were performed on the BI-200SM Laser Light Scattering System (Brookhaven). The morphologies of the nanoaggregates were investigated using a Tecnai G^2S-Twin F20 TEM at an accelerating voltage of 200 kV.

2.2. Synthesis

2.2.1. Synthesis of Compounds **2** and **3**

The intermediates **2** and **3** were prepared according to the previously reported method [27], with all their characterization data matching the literature data.

2.2.2. Synthesis of Compound **TPE-ND**

Compound **3** (0.34 g, 1.0 mmol) and 2-hydroxy-1-naphthaldehyde (0.17 g, 1.0 mmol) in ethanol (30 mL) were refluxed for 10 min, then an orange solid was precipitated. The product was filtered and washed several times with ethanol and then collected with a high yield of 94 %. Mp: 203–204 °C. ^{1}H NMR (400 MHz, DMSO-d_6): δ 15.75 (d, J = 5.1 Hz, 1H), 9.59 (d, J = 5.2 Hz, 1H), 8.45 (d, J = 8.5 Hz, 1H), 7.91 (d, J = 9.2 Hz, 1H), 7.78 (d, J = 7.9 Hz, 1H), 7.52 (t, J = 7.7 Hz, 1H), 7.43 (d, J = 8.2 Hz, 2H), 7.34 (t, J = 7.4 Hz, 1H), 7.22 –7.11 (m, 9H), 7.10 – 6.94 (m, 9H). (Fig. S6). ^{13}C NMR (101 MHz, DMSO-d_6): δ 171.53, 155.12, 143.61, 143.51, 142.15, 141.94, 141.39, 140.32, 137.41, 133.62, 132.42, 131.20, 131.14, 131.09, 129.43, 128.53, 128.46, 128.35, 128.26, 127.19, 127.12, 127.07, 127.03, 123.92, 122.79, 120.81, 120.29,

108.99. (Fig. S7). HRMS (MALDI-TOF) m/z: $[M+H]^+$ Calcd for $C_{37}H_{27}NO$ 502.2126; Found 502.2176 (Fig. S8).

2.2.3. Synthesis of Compound **TPE-NDB**

The corresponding boron complex **TPE-NDB** was synthesized by reaction of **TPE-ND** with boron trifluoride etherate in the presence of triethylamine. The residual crude product was purified by silica gel chromatography to obtain a yellow boron complex. Yield: 89%. Mp: 215–216 °C ^{1}H NMR (400 MHz, $CDCl_3$): δ 9.06 (s, 1H), 8.10 (d, *J* = 9.1 Hz, 1H), 8.06 (d, *J* = 8.4 Hz, 1H), 7.85 (d, *J* = 8.0 Hz, 1H), 7.70 – 7.62 (m, 1H), 7.50 (t, *J* = 7.5 Hz, 1H), 7.36 (d, *J* = 8.3 Hz, 2H), 7.32 – 7.26 (m, 2H), 7.20 – 7.04 (m, 16H). (Fig. S9).^{13}C NMR (101 MHz, $CDCl_3$): δ 162.63, 157.40, 144.85, 143.32, 143.19, 143.14, 142.35, 140.90, 140.83, 139.46, 132.54, 131.46, 131.35, 131.27, 131.22, 129.76, 129.43, 128.08, 127.97, 127.86, 127.68, 126.93, 126.75, 126.69, 125.09, 122.78, 120.51, 119.16, 108.74. (Fig. S10). ^{19}F NMR (376 MHz, $CDCl_3$): δ -134.95, -134.98, -135.03, -135.06. (Fig. S11). HRMS (MALDI-TOF) m/z: $[M+H]^+$ Calcd for $C_{37}H_{26}BF_2NO$ 550.2109; Found 550.2183 (Fig. S12).

2.3. Preparation of the samples for AIE measurements

A 10^{-3} M stock solution of target molecules in THF was prepared. Aliquots (100 μL) of the stock solution were added to 10 mL volumetric flasks and diluted to volume with water and THF in the proper ratios under sonication at room temperature, the concentration was maintained at 1.0×10^{-5} M. The fluorescence emission spectral measurement of the mixture was performed immediately.

2.4. Preparation of the samples for mechanofluorochromism study

The grinding powders were obtained by grinding the as-synthesized crystals with a pestle in the mortar. The fumed samples were prepared by fuming the grinding powders with DCM for 2 min.

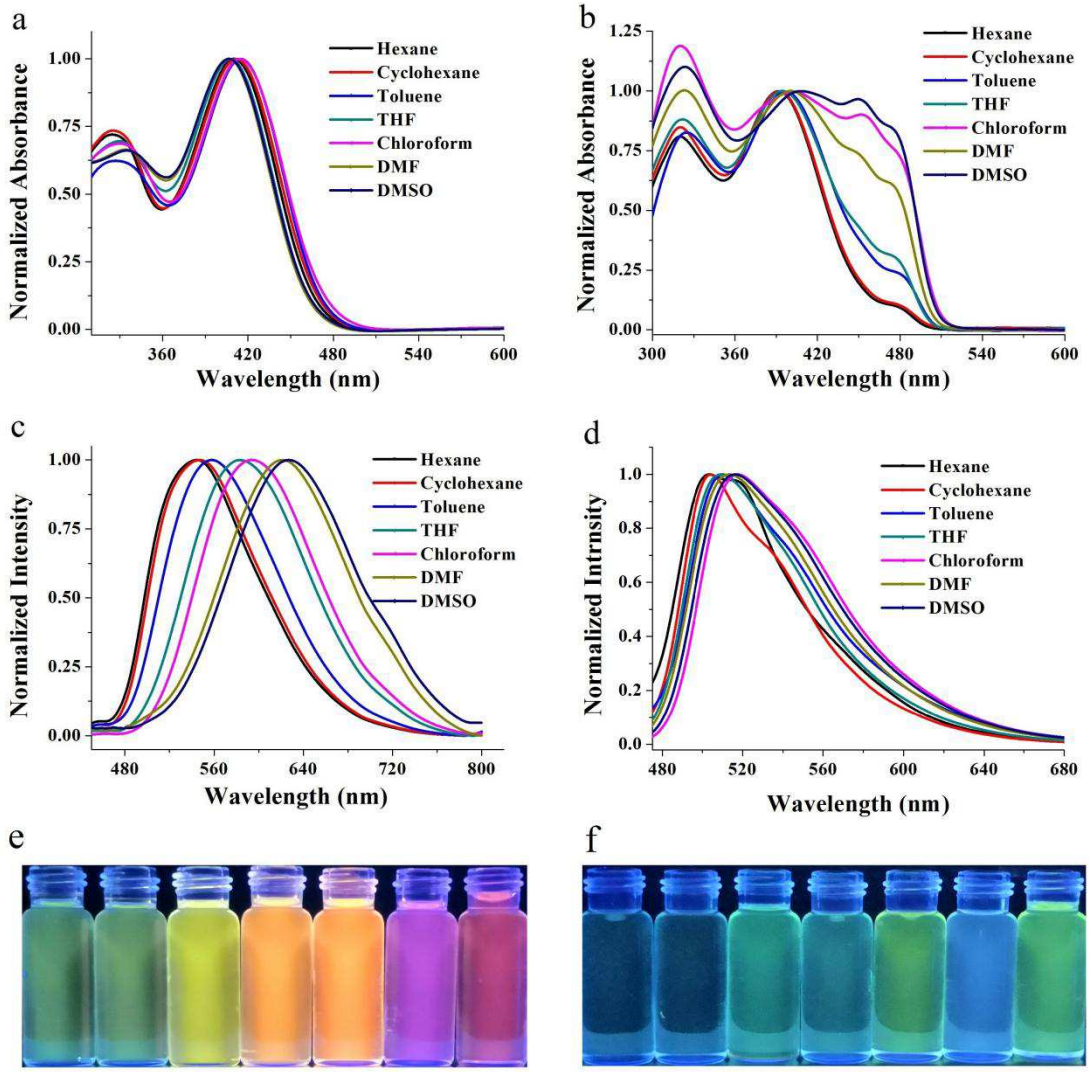

Fig. 1. Normalized UV-vis absorption of **TPE-NDB** (a) and **TPE-ND** (b), and PL spectra of **TPE-NDB** (c) and **TPE-ND** (d) excited at 400 nm in different solvents (1.0 × 10^{-5} mol L^{-1}). Photographs of **TPE-NDB** (e) and **TPE-ND** (f) taken under UV illumination in different solvents, from left to right: hexane, cyclohexane, toluene, THF, chloroform, DMF, and DMSO.

3. Results and discussion

3.1. Synthesis

The target ligand is conveniently synthesized by the reaction of compound **3** with 2-hydroxy-1-naphthaldehyde in a high yield (94%). **TPE-ND** was allowed to react with

boron trifluoride etherate in the presence of triethylamine to give corresponding boron complex **TPE-NDB** with yield 89%.

3.2. Optical Properties in solution

In order to probe the optical properties of Schiff base ligand and boron complex in solvents with different polarities, UV-vis and fluorescence spectroscopy were carried out. The UV-vis absorption and fluorescence emission spectra were shown in Fig. 1, and the corresponding photophysical data are summarized in Table S1. The UV-vis absorption spectra of **TPE-NDB** (Fig. 1a) shown an absorption band from λ = 280nm to 350 nm. This band did not shift with increasing polarity of the solvents, which was attributed to π–π* local electron transitions of the conjugate system. The absorption band at λ = 360 – 520 nm exhibited a trend of red-shifted with the increasing solvent polarity, assigned to the ICT transition. From the absorption spectra of the ligand (Fig. 1b), **TPE-ND** also had two main absorption bands at *ca.* 330 nm and *ca.* 410 nm in different solvents, which can be assigned to the π-π* transition of the conjugated system and ICT transitions, respectively [28]. The solvent-dependent PL spectra of TPE-NDB were shown in Fig.1c, it is clear that the emission bands were dramatically red-shifted with increasing solvent polarity, and was accompanying with large Stokes shift. In hexane, the **TPE-NDB** emission band located at 544 nm and its Stokes shift was 5948 cm^{-1}, and with increasing polarity of the solvents, its emission band and Stokes shift reached 627 nm and 8621 cm^{-1} in DMSO, respectively. The result suggests that ICT transitions of **TPE-NDB** take place at excited state in more polar solvents [29]. It is worth mentioning that the fluorescence spectra of **TPE-NDB** became structured in non-polar solvents, such as hexane and cyclohexane, which indicated that the emission was typical from the locally excited (LE) state [30]. The

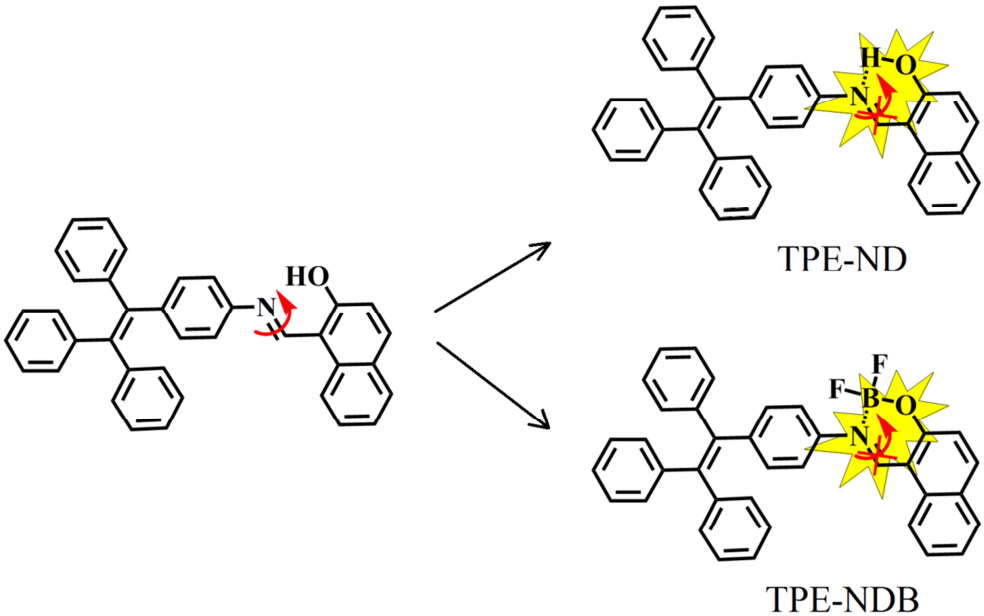

Scheme 2. Illustration of inhibited C=N isomerization by hydrogen bonding (**TPE-ND**) and N, O-chelated boron complex (**TPE-NDB**)

PL spectra of **TPE-ND** ligand demonstrated a small red shift of emission upon increased solvent polarity. The emission band located at 503 nm in hexane, and reached to 516 nm in DMSO. The results indicated that the ICT propterty of ligand was weaker than boron complex. Moreover, **TPE-NDB** exhibited significantly red-shifted absorption bands as compared with the ligand in the same solution. For example, in THF the emission peak of ligand was centered at 509 nm (Φ_f = 0.03), by contrast, the emission band of boron chelated complex localed at 583 nm (Φ_f = 0.08), displayed a large red-shift of 74 nm. The extended π-conjugation skeleton produced by the embedded boron atom was responsible for this phenomenon (Scheme 2) [31].

In order to obtain a better insight of spectroscopic properties, we calculated frontier molecular orbital by using the density functional theory (DFT) method at the B3LYP/6-31G* level with the Gaussian 09W program. Fig. 2 showed the electron

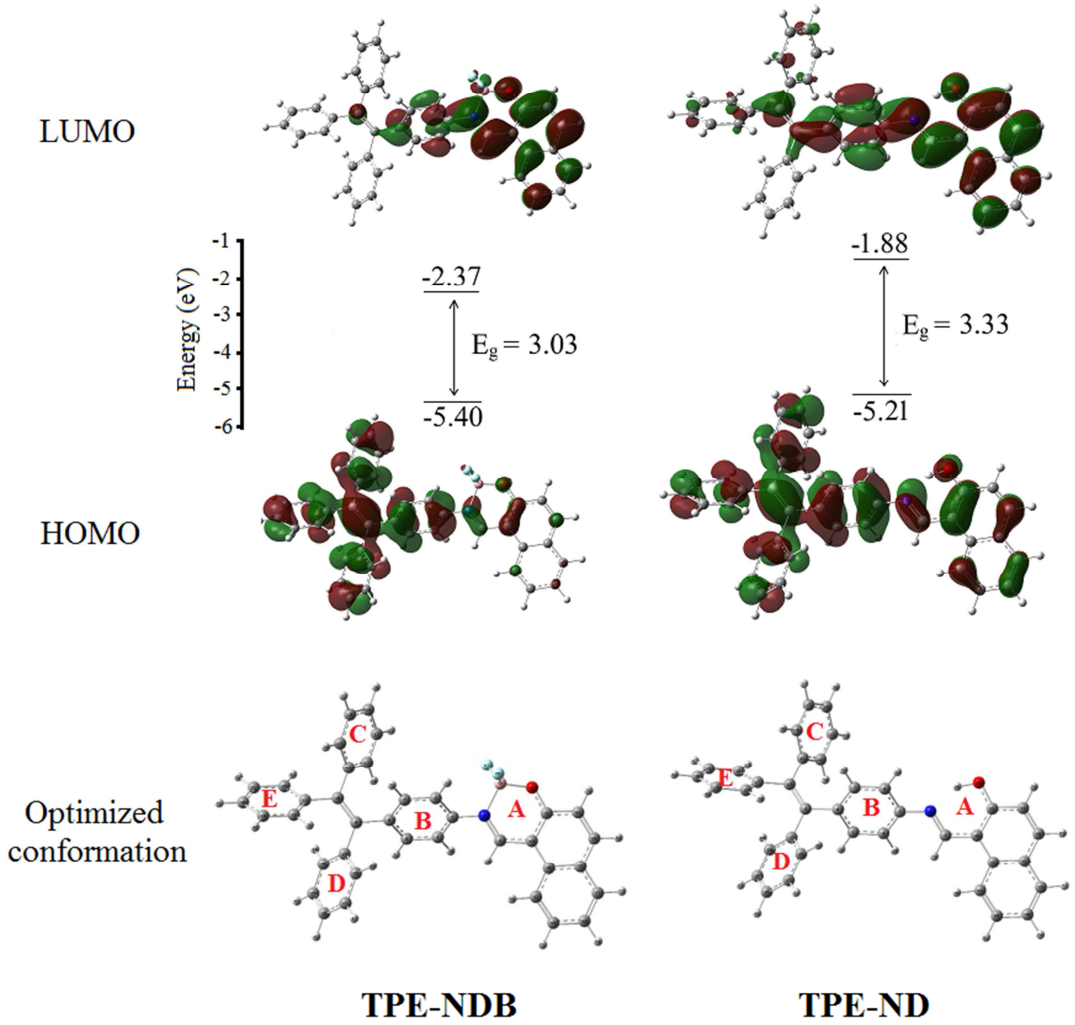

Fig. 2. Energy levels of HOMO and LUMO, energy gaps, and electron cloud distributions calculated by the B3LYP/6-31G* program, and the optimized conformation structures of **TPE-NDB** and **TPE-ND**.

distribution of the highest occupied molecular orbital (HOMO) and the lowest occupied molecular orbital (LUMO) of **TPE-NDB** and **TPE-ND** [32]. It was found that the HOMO of **TPE-NDB** mostly localized on the major donor (i.e., the TPE unit), while the LUMO shifts to the right part of the molecule because of the strong electron withdrawing ability of the naphthalene boron moiety in terms of its strong push–pull structure, implying that light excitation would lead to ICT from the donor unit to the

acceptor unit as occurs in most D–A type molecules. The HOMO of **TPE-ND** ligand was mostly located at the whole molecule, and the LUMO was mainly distributed at naphthalene boron unit, resulting in a weak ICT performance. This information is helpful in understanding the absence of the MFC behavior of **TPE-ND**. The asymmetrical electron cloud distribution of the HOMO and LUMO of **TPE-NDB** resulted in an energy gap of 3.03 eV, which was lower than ligand alone (3.33eV), further confirming the ICT property of **TPE-NDB** was stronger than **TPE-ND**. The decrease in the HOMO−LUMO energy band gap of **TPE-NDB** boron complex compared to the ligand was due to that the C=N isomerization was inhibited by the complexation of B(III) , produced more rigid boron-bridged π-framework (Scheme 2). It was assumed that more rigid structure significantly reduces the energies of singlet excited states and a much lower singlet-triplet (ST) energy splitting for **TPE-NDB**. The optimized geometries of **TPE-NDB** and **TPE-ND** showed twisted nonplanar shapes, respectively. Dihedral angles between the O−H···N hydrogen bonds ring A and phenyl group B in **TPE-ND** was 32.2°, and it increases to 41.2° after the covalently bridged C=N structure by N, O-chelated BF_2 of **TPE-NDB**. The dihedral angles between phenyl rings in tetraphenylethene units, including B–C, B–D, and B–E remain unchanged (Tab. S3). The introduction of boron group thus leaded to the enhanced the degree of molecular distortions. The above theoretical results further illustrate the occurrence of the ICT process, which is consistent with the observed optical property (Fig. 1). The features of twisted spatial conformation and ICT transition of **TPE-NDB** and **TPE-ND** may endow them with vivid color emission in the condensed/solid state [33].

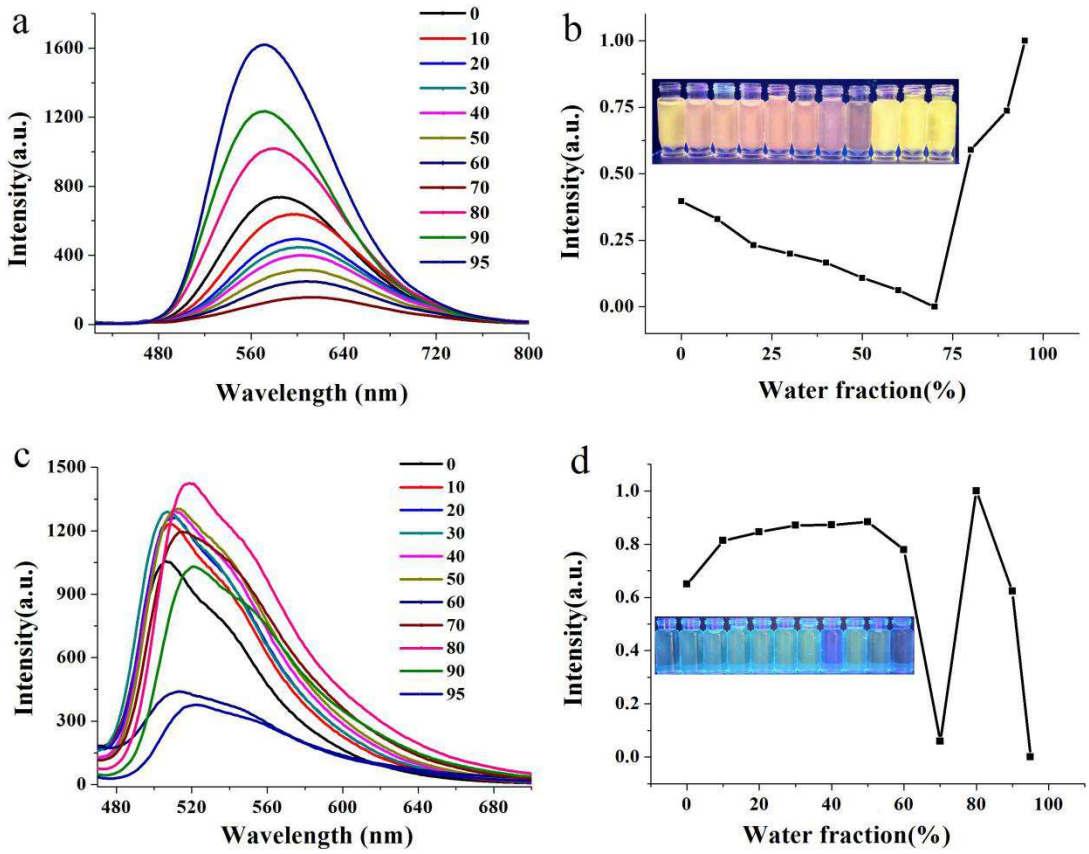

Fig. 3. PL spectra of **TPE-NBD** (a) and **TPE-ND** (c) in THF–water with different water fractions (vol., 0-95%), λ_{ex} = 400 nm. Normalized fluorescent emission intensities of **TPE-NBD** (b) and **TPE-NB** (d) in THF–water with different f_w. The inset graphs in (b) and (d) are the solutions of **TPE-NBD** and **TPE-ND** in THF-water under irradiation of UV lamp at 365 nm, from left to right (f_w): 0%, 10%, 20%, 30%, 40%, 50%, 60%, 70%, 80%, 90%, 95%.

3.3. Aggregation induced emission (AIE)

The AIE effects of the synthesized ligand and boron complex were examined by comparing the fluorescence emission spectra of THF/H_2O solution with different water fraction (f_w, the volume percentage of water). As shown in Fig. 3, in dilute THF solution, the emission band of **TPE-NDB** was broad with a center at 586 nm, and Φ_f is very low (0.08), which might be due to active intramolecular rotations of the

compound. The boron complex **TPE-NDB** served as relaxation channels for the excited state in this situation. When an appropriate amount of water was added to the THF solution, the emission peaks decreased and eventually disappeared. The fluorescence quenching was attributed to the ICT effect in polar solvent for **TPE-NDB** with D–A structure [15e]. When f_w was above 70%, **TPE-NDB** displayed a sudden increase in the emission intensity due to molecular aggregation. As f_w was 95%, the emission peak located at 571 nm, and the PL intensity is approximately 2.5 times higher than that in the pure THF. The fluorescence enhancement phenomenon could be ascribed to the restriction of the intramolecular rotations, which blocked the non-irradiative channels and caused clear enhancement of emission in aggregated states [15]. The emission of **TPE-ND** exhibited an enhancement in the emission intensity with gradual increase from f_w = 0% to f_w = 50%, and showed a rapid decrease at f_w = 70%. At an f_w of 80%, a significant increase in the emission intensity was observed, which can be attributed to the AIE effect caused by the formation of molecular aggregates when water is added into the THF solution. The PL intensity for **TPE-ND** showed a zig-zag pattern (Fig. 1d). This phenomenon was often observed in the determination of the AIE effect, but the reasons remain unclear [34]. There are two possible explanations for this phenomenon [35]. First, when water is added, the solute molecules can aggregate into crystal particles or amorphous particles suspensions [36]. The crystal particles suspension results in an enhancement in the PL intensity, in contrast, the amorphous particles suspension leads to a decrease of PL intensity. Second, only the molecules on the surface of the nanoparticles emitted light after the aggregation, which lead to a decrease in PL intensity. However, the restriction of intramolecular rotations of the aromatic rings in the aggregation state could enhance light emission. The net output of these antagonistic processes depends

on which process plays a key role in affecting the fluorescent behavior of the aggregated molecules [37]. Thus, the measured PL intensity often shows no regularity in high water content. To further reveal the AIE behavior of **TPE-NBD** and **TPE-ND**, dynamic light scattering (DLS) and transition electron microscopy (TEM) were employed to study the microstructures in the aggregate state. As shown in Fig. S1, **TPE-NDB** aggregates were obtained when f_w was 95%, with the size from 20 to 120 nm. When f_w was 80%, **TPE-ND** aggregates also emerged with the size of 20−150 nm. The TEM images indicated that the nanoparticles were in amorphous state both for **TPE-NDB** and **TPE-ND** (Fig. S2). These results clearly implied that **TPE-NBD** and **TPE-ND** are AIE-active molecules.

In many works, the Schiff base ligands don't possess AIE behavior due to the intramolecular rotations of C=N bond, which could produce the non-irradiative channels [38]. In this work, the Schiff base ligand **TPE-ND** exhibited AIE characteristics, although the fluorescence is weak. This phenomenon could be ascribed to the intramolecular hydrogen bond O−H···N is formed to yield a six-membered pseudo ring, such structure helps the molecules to further rigidify their conformation and to restrict molecular vibration, thus producing the AIE feature (Scheme 2). When the covalently bridged C=N structure by N, O-chelated BF_2, the rigid molecular structure is improved. The rigid boron-bridged π-frameworks tend to undergo very rapid nonradiative decay and intensify the AIE performance.

3.4. Mechanochromic properties

Generally, the compound possessing non-planar geometries and D-A conjugated systems with ICT properties is expected to undergo MFC behavior. The fluorescent performance of the solid sample **TPA-NDB** in response to external pressure was investigated. The crude product was purified on a silica-gel column to afford a yellow

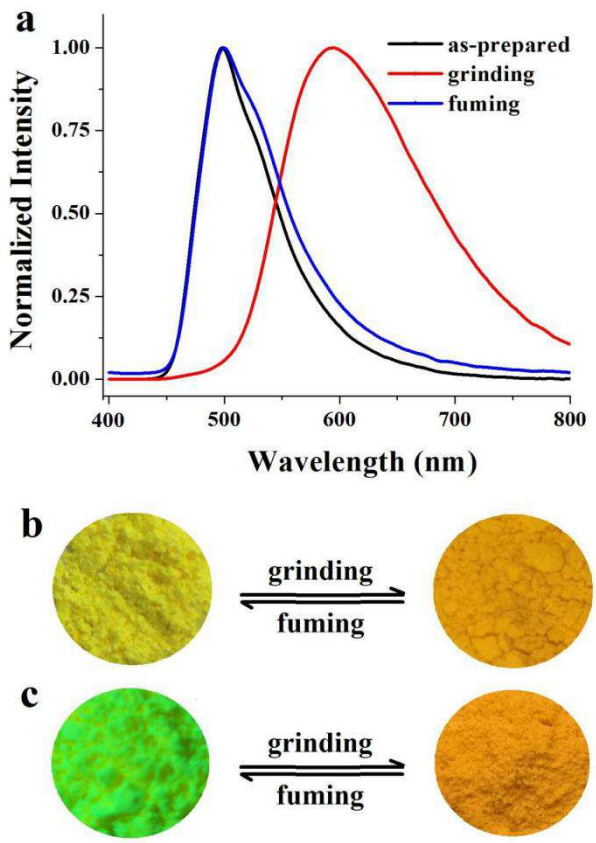

Fig. 4. (a) Normalized fluorescent spectra of **TPE-NDB** in different solid-states: as-prepared, grinding and fuming, λ_{ex} = 365 nm. Photographs of **TPE-NDB** color changes upon grinding and fuming stimuli by naked eyes (b) and under UV light (365 nm) (c).

powder. As shown in Fig. 4, the as-prepared **TPE-NBD** powder demonstrated bright green emission under 365 nm UV-light illumination. Interestingly, after grinding with a mortar and pestle, the powder changed its emission color into orange. The force-induced color switch could be fully restored by fuming with DCM for 2 minutes at room temperature. The fluorescence converted rapidly to bright green, similar to their original powders. The color changes could be observed with the naked eye (Fig. 4b). In addition, this process of fluorescence color change could be repeated many times (Fig. S3). The dye displayed excellent reversibility without any fatigue in response

throughout the six cycles, demonstrating the obvious and reversible MFC behavior of the **TPE-NDB**. The PL spectra measurement was applied to monitor such a reversible color switching under external stimuli. As depicted in Fig. 4a, the emission peak of as-prepared powder centered at 498 nm, and red-shifted to 595 nm after grinding, which suggested that the grinding treatment has induced a significant spectral red-shift of 97 nm. The Φ_f of as-prepared and ground sample for **TPE-NDB** in solid state were 0.35 and 0.19, respectively (Tab. S2). High intensity solid-state emission and the prominent color contrast before and after the application of mechanical stimulus are very significant for the effective application of MFC materials. The MFC properties of **TPE-ND** were also tested by grinding treatment. However, there was almost no change in the main fluorescence peak of the compound **TPE-ND** and could not lead to the color change before and after grinding, suggesting that **TPE-ND** has no MFC activity. These observations are consistent with the assumption that while boron has immensely enhanced the rigid molecular structure since it can result in the increase of molecular distortion degree and ICT feature, which endows **TPE-NDB** with obvious MFC behavior, in contrast, the ligand **TPE-ND** has no MFC property. These phenomena are accord with the observed optical property and DFT result.

The luminescent decay profiles of **TPE-NDB** in solid state were carried out (Fig. S5) and the corresponding data were illustrated in Tab. S2. The lifetime of **TPE-NDB** and **TPE-ND** were 4.53 ns and 2.10 ns, respectively. The excited-state decay of as-prepared **TPE-NDB** fitted one exponential function. The data of ground sample **TPE-NDB** fitted a double-exponential decay, which revealed the mixture of two distinguished emission states in the amorphous phase.

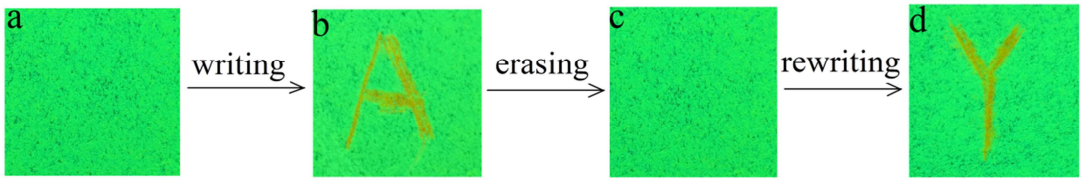

Fig. 5. Photos of the luminescence writing/erasing process of **TPE-NDB** on filter papers under UV light (365 nm): (a) fluorescence emission of as-synthesized powder; (b) mechanochromic fluorescence of the letter of "A" was written with a spatula; (c) the paper was erased by vapor fuming (the letter "A" becoming invisible); (d) rewritable mechanochromic fluorescence of the letter of "Y" generated with a spatula.

Switchable mechanochromic dye of **TPE-NDB** with a large shift of 97 nm prompts us to evaluate it as a kind of smart material with numerous potential applications. An example of such applications is demonstrated in Fig. 5, after being simply pressed by streaking a metal spatula on a piece filter paper with sprayed as-synthesized powder, an orange letter appeared on the bright green background due to the amorphization of **TPE-NDB** in the written "A" area under UV light illumination (Fig. 5b). Interestingly, after vapor fuming the letter "A" can be merged in the background because of the crystallization of **TPE-NDB** in area of "A" (Fig. 5c), and a clear orange letter "Y" can be written again (Fig. 5d). Such writing and erasing process can be repeated many times through repeating writing and fuming processes. On the basis of its excellent MFC properties, **TPE-NDB** may be utilized as optical recording materials.

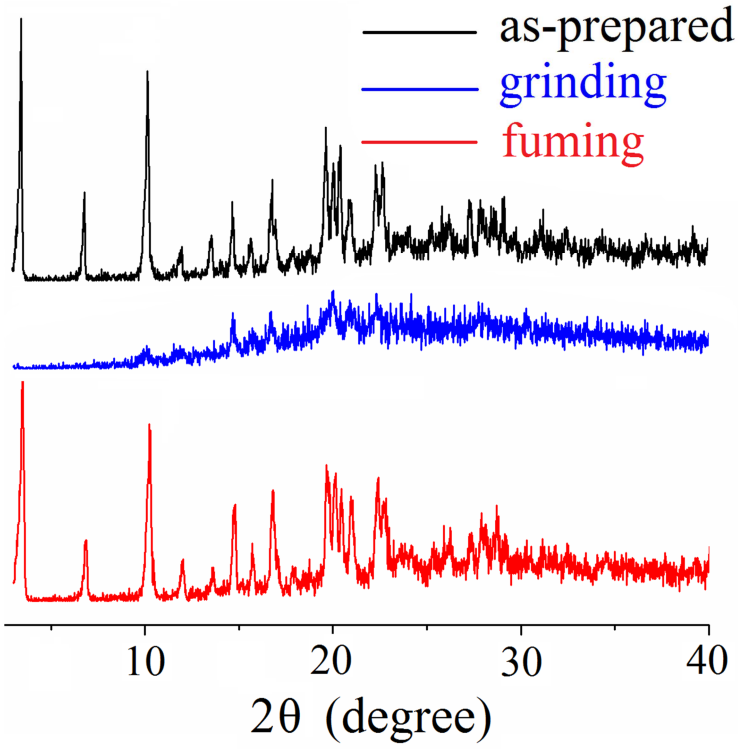

Fig. 6. XRD patterns of **TPE-NDB** in different solid-states: as-prepared, grinding and fuming.

With the aim of getting insight into the mechano-induced emission color changes, powder X-ray diffraction (XRD) was used to study the synthesized **TPE-NDB** in different solid states. As shown in Figure 6, many sharp and intense reflection peaks were observed in the diffraction pattern of the untreated sample, indicating that the as-prepared **TPE-NDB** was well-ordered arrangement crystalline structure. In sharp contrast, all of the diffraction peaks displayed diffuse and depressed reflections after grinding, verifying that the ground sample was amorphous. The transformation from the crystalline structure into an amorphous state took place under an external force and, thus, led to a change in the emitting color from bright green to orange. When fumed with DCM, sharp reflection peaks resemble to those of the as prepared powder emerge out, suggesting the ground sample can be readily converted back into an ordered crystalline lattice. In addition, the ^{1}H NMR spectrum of **TPE-NDB** after

grinding treatment was shown in Fig. S13, the result is similar with that the as-prepared sample obtained (Fig. S9), implying that **TPE-NDB** converts the emission color without changing its chemical structure during grinding process. Accordingly to these results, the mechanochromism of **TPE-NDB** should be attributed to the crystalline-amorphous phase transformations, which greatly influences photophysical properties.

4. Conclusions

In summary, an efficient strategy to design novel tetraphenylethene-based Schiff base ligand **TPE-ND** and the corresponding boron complex **TPE-NDB** were developed. The ligand **TPE-ND** showed a typical ICT characteristic in addition to an AIE behavior. The boron complex **TPE-NDB** resulted in enhanced and red-shifted emission, more dramatic solvatochromism, bright AIE phenomenon, and reversible high contrast MFC behavior due to the inhibition of C=N isomerization in ligands. Upon grinding the as-prepared sample of **TPE-NDB**, the emission color changed from bright green to orange, accompanied with the remarkable spectral shift from 498 to 595 nm. It should be mentioned that such a large red-shift of 97 nm during MFC process has been rarely reported for organic compounds. Moreover, the ground powder of **TPE-NDB** that emitted orange could be switched into its as-prepared state emitting bright green light by fuming with DCM for 2 min. The results of this work will facilitate the rational design of new MFC dyes with high−contrast performance and the exploration of their potential applications in high-tech fields.

Conflict of Interest

The authors declare no conflict of interest.

Acknowledgements

We are grateful to the Program for Innovative Research Team of Science and Technology in the University of Henan Province (18IRTSTHN004), and Anyang Normal University Program (AYNU-2017-B16, AYNUKP-2018-B20) for financial support of this research.

References

[1] Chen Q, Wang JX, Yang F, Zhou D, Bian N, Zhang XJ, Yan CG, Han BH. Tetraphenylethylene-based fluorescent porous organic polymers: preparation, gas sorption properties and photoluminescence properties. J Mater Chem 2011; 21: 13554−60.

[2] Mei J, Hong YN, Lam JWY, Qin AJ, Tang YH, Tang BZ. Aggregation-induced emission: the whole is more brilliant than the parts. Adv Mater 2014; 26: 5429−79.

[3] (a) Liu B, Dan T, Bazan GC. Collective response from a cationic tetrahedral fluorene for label-free DNA detection. Adv Funct Mater 2007; 17: 2432−8;

(b) Toal SJ, Jones KA, Magde D, Trogler WC. Luminescent silole nanoparticles as chemoselective sensors for Cr (VI). J Am Chem Soc 2005; 127: 11661−5;

(c) Wu YT, Kuo MY, Chang YT, Shin CC, Wu TC, Tai CC, et al. Synthesis, structure, and photophysical properties of highly substituted 8,8a-dihydrocyclopenta[a]indenes. Angew Chem Int Ed 2008; 47: 9891−4.

[4] Sun H, Liu S, Lin W, Zhang KY, Lv W, Huang X, et al. Smart responsive phosphorescent materials for data recording and security protection. Nat Commun 2014; 5: 4601/1–4601/9.

[5] Wang J, Mei J, Hu R, Sun JZ, Qin A, Tang BZ. Click synthesis, aggregation-induced emission, E/Z isomerization, self-Organization, and multiple chromisms of pure stereoisomers of a tetraphenylethene-cored luminogen. J Am Chem Soc 2012; 134: 9956−66

[6] Luo J, Xie Z, Lam JWY, Cheng L, Chen H, Qiu C, et al. Aggregation-induced emission of 1-methyl- 1, 2, 3, 4, 5-pentaphenylsilole. Chem Commun 2001; 18: 1740–1.

[7] Wang ZM, Nie H, Yu ZQ, Qin AJ, Zhao ZJ, Tang BZ. Multiple stimuli-responsive and reversible fluorescence switches based on a diethylamino-functionalized tetraphenylethene. J Mater Chem C 2015; 3: 9103–11.

[8] (a) Tong H, Dong YQ, Hong YN, Haussler M, Lam JWY, Sung HHY et al. Aggregation-induced emission: effects of molecular structure, solid-state conformation, and morphological packing arrangement on light-emitting behaviors of diphenyldibenzofulvene derivatives. J Phys. Chem C 2007; 111: 2287–94;

(b) Gu XG,Yao JJ, Zhang GX, Yan YL, Zhang C, Peng Q, et al. Adv Funct Mater 2012; 22: 4862-72;

(c) He ZK, Zhang LQ, Mei J, Zhang T, Lam JWY, Shuai ZG, et al. Polymorphism-dependent and switchable emission of butterfly-like bis(diarylmethylene)-dihydroanthracenes. Chem Mater 2015; 27: 6601−7.

[9] (a) Zhang X, Chi Z, Li H, Xu B, Li X, Zhou W, et al. Piezoflfluorochromism of an aggregation-induced emission compound derived from tetraphenylethylene. Chem Asian J 2011; 6: 808−11;

(b) Dong YJ, Xu B, Zhang JB, Tan X, Wang LJ, Chen JL, et al. Piezochromic luminescence based on the molecular aggregation of 9,10-Bis((E)-2-(pyrid-2-yl)vinyl)anthracene. Angew Chem Int Ed 2012; 51: 10782−5;

(c) Sagara Y, Yamane S, Mutai T, Araki K, Kato T. A stimuli-responsive, photoluminescent, anthracene-based liquid crystal: emission color determined by thermal and mechanical processes. Adv Funct Mater 2009; 19: 1869−75.

[10] Shi XY, Wang H, Han TY, Feng X, Tong B, Shi JB, et al. A highly sensitive, single selective, real-time and "turn-on"fluorescent sensor for Al^{3+} detection in aqueous media. J Mater Chem 2012; 22: 19296−302.

[11] Hu R, Leung NLC, Tang BZ. AIE macromolecules: syntheses, structures and functionalities. Chem Soc Rev 2014; 43: 4494−562.

[12] (a) Luo X, Li J, Li C, Heng L, Dong Y,Liu Z, et al. Reversible switching of the emission of diphenyldibenzofulvenes by thermal and mechanical stimuli. Adv Mater 2011; 23: 3261–5;

(b) Yuan WZ, Tan YQ, Gong YY, Lu P, Lam JWY, Shen XY, et al. Synergy between twisted conformation and effective intermolecular interactions: strategy for efficient mechanochromic luminogens with high contrast. Adv Mater 2013; 25: 2837–43.

[13] (a) Chi Z, Zhang X, Xu B, Zhou X, Ma C, Zhang Y, et al. Recent advances in organic mechanofluorochromic materials. Chem Soc Rev 2012; 41: 3878–96;

(b) Zhang X, Chi Z, Zhang J, Li H, Xu B, Li X, et al. Piezoflfluorochromic properties and mechanism of an aggregation-induced emission enhancement compound containing N-hexyl-phenothiazine and anthracene moieties. Phys Chem B 2011; 115: 7606–11;

(c) Li H, Chi Z, Xu B, Zhang X, Li X, Liu S, et al. Aggregation-induced emission enhancement compounds containing triphenylamine-anthrylenevinylene and tetraphenylethene moieties. J Mater Chem 2011; 21: 3760–7;

(d) Lu Q, Li X, Li J, Yang Z, Xu B, Chi Z, et al. Influence of cyano groups on the properties of piezofluorochromic aggregation-induced emission enhancement compounds derived from tetraphenylvinyl-capped ethane. J Mater Chem C 2015; 3: 1225–34;

(e) Xu B, Chi Z, Zhang J, Zhang Z, Li H, Li X, et al. Piezofluorochromic and aggregation-induced-emission compounds containing triphenylethylene and tetraphenylethylene moieties. Chem Asian J 2011; 6: 1470–8.

[14] (a) Liu W, Wang Y, Sun M, Zhang D, Zheng M, Yang W. Alkoxy-position effects on piezofluorochromism and aggregation-induced emission of 9,10-bis(alkoxystyryl)anthracenes. Chem Commun 2013; 49: 6042–4;

(b) Zheng M, Zhang D, Sun M, Li Y, Liu T, Xue S, et al. Cruciform 9,10-distyryl-2,6-bis(p-dialkylamino-styryl)anthracene homologues exhibiting alkyl length-tunable piezochromic luminescence and heat-recovery temperature of ground states. J Mater Chem C 2014; 2: 1913–20;

(c) Bu L, Sun M, Zhang D, Liu W, Wang Y, Zheng M, et al. Solid-state fluorescence properties and reversible piezochromic luminescence of aggregation-induced emission-active 9,10-bis[(9,9-dialkylfluorene-2-yl)vinyl]anthracenes. J Mater Chem C 2013; 1: 2028–35;

(d) Wang Y, Liu W, Bu L, Li J, Zheng M, Zhang D, et al. Reversible piezochromic luminescence of 9,10-bis[(N-alkylcarbazol-3-yl)vinyl]anthracenes and the dependence on N-alkyl chain length. J Mater Chem C 2013; 1: 856–62.

[15] (a) Gao H, Xu D, WangY, Wang Y, Liu X, Han A, et al. Effects of alkyl chain length on aggregation-induced emission, self-assembly and mechanofluorochromism of tetraphenylethene modified multifunctional β-diketonate boron complexes. Dyes Pigm 2018; 150: 59–66;

(b) Zhou L, Xu D, Gao H, Han A, Liu X, Zhang C,et al. Triphenylamine functionalized β -Ketoiminate boron complex exhibiting aggregation-induced emission and mechanofluorochromism. Dyes Pigm 2017; 137: 200-7;

(c) Gao H, Xu D, Liu X, Han A, Zhou L, Zhang C, et al. Tetraphenylethene modified β-ketoiminate boron complexes bearing aggregation-induced emission and mechanofluorochromism. RSC Adv 2017; 7: 1348–56;

(d) Gao H, Xu D, Liu X, Han A, Zhou L, Zhang C, et al. Tetraphenylethene-based β-diketonate boron complex: Efficient aggregation-induced emission and high contrast mechanofluorochromism. Dyes Pigm 2017; 139: 157–65;

(e) Zhou L, Xu D, Gao H, Han A, Yang Y, Zhang C, et al. Effects of cyano groups on the properties of thiazole-based b-ketoiminate boron complexes: aggregation-induced emission and mechanofluorochromism. RSC Adv 2016; 6: 69560–8;

(f) Wang Y, Xu D, Gao H, Wang Y, Liu X, Han A, et al. Twisted Donor−Acceptor Cruciform Luminophores Possessing Substituent-Dependent Properties of Aggregation-Induced Emission and Mechanofluorochromism. J Phys Chem C 2018; 122: 2297−306.

[16] (a) Ooyama Y, Kagawa Y, Fukuoka H, Ito G, Harima Y. Mechanofluorochromism of a series of benzofuro [2, 3-c] oxazolo [4, 5-a] carbazole-type fluorescent dyes. Eur J Org Chem 2009; 5321–6;

(b) Ooyama Y, Harima Y. Molecular design of mechanofluorochromic dyes and their solid-state fluorescence properties. J Mater Chem 2011; 21: 8372–80.

[17] (a) Lim SJ, An BK, Jung SD, Chung MA, Park SY. Photoswitchable organic nanoparticles and a polymer film employing multifunctional molecules with enhanced fluorescence emission and bistable photochromism. Angew Chem Int Ed 2004; 43: 6346−50;

(b) Kishimura A, Yamashita T, Yamaguchi K, Aida T. Rewritable phosphorescent paper by the control of competing kinetic and thermodynamic self-assembling events. Nat Mater 2005; 4: 546−9.

[18] (a) Shen XY, Wang YJ, Zhao E, Yuan WZ, Liu Y, Lu P, et al. Effects of substitution with donor−acceptor groups on the properties of tetraphenylethene trimer: aggregation-induced emission, solvatochromism, and mechanochromism. J Phys Chem C 2013; 117: 7334−47;

(b) Ma CP, Xu BJ, Xie GY, He JJ, Zhou X, Peng BY, et al. An AIE-active luminophore with tunable and remarkable fluorescence switching based on the piezo and protonation–deprotonation control. Chem Commun 2014; 50: 7374–7;

(c) Aldred MP, Zhang GF, Li C, Chen G, Chen T, Zhu MQ. Optical properties and red to near infrared piezo-responsive fluorescence of a tetraphenylethene-perylenebisimide-tetraphenylethene triad. J Mater Chem C 2013; 1: 6709–18.

[19] (a) Zhao J, Peng J, Chen P, Wang H, Xue P, Lu R. Mechanofluorochromism of difluoroboron β-ketoiminate boron complexes functionalized with benzoxazole and benzothiazole. Dyes Pigm 2018; 149, 276–83;

(b) Zhao Y, Lin H, Chen M, Yan D. Niflumic anion intercalated layered double hydroxides with mechano-induced and solvent-responsive luminescence. Ind Eng Chem Res 2014; 53: 3140−47;

(c) Li Y, Zhuang Z, Lin G, Wang Z, Shen P, Xiong Y, et al. A new blue AIEgen based on tetraphenylethene with multiple potential applications in fluorine ion sensors,

mechanochromism, and organic light-emitting diodes. New J Chem 2018; 42: 4089-94;

(d) Chen M, Chen R, Shi Y, Wang J, Cheng Y, Li Y, et al. Malonitrile-functionalized tetraphenylpyrazine: aggregation-induced emission, ratiometric detection of hydrogen sulfide, and mechanochromism. Adv Funct Mater 2018; 28: 1704689;

(e) Lin C, Liu Y, Peng S, Shinmyozu T, Yang J. Excimer−monomer photoluminescence mechanochromism and vapochromism of pentiptycene -containing cyclometalated platinum(II) complexes. Inorg Chem 2017; 56: 4978-89.

[20] Das P, Linert W. Schiff base-Derived Homogeneous and Heterogeneous Palladium Catalysts for the Suzuki−Miyaura Reaction. Coord Chem Rev 2016; 311: 1−23.

[21] Feng L, Shi W, Ma J, Chen Y, Kui F, Hui Y, et al. A novel thiosemicarbazone Schiff base derivative with aggregation-induced emission enhancement characteristics and its application in Hg^{2+} detection. Sensor Actuat B Chem 2016; 237: 563−9.

[22] Al-Zoubi W, Al-Hamdani AAS, Kaseem M. Synthesis and antioxidant activities of schiff bases and their complexes: a review. Appl Organomet Chem 2016; 30: 810−7.

[23] (a) G Liu, Yang MD, Wang LK, Zheng J, Zhou HP, Wu JY et al. Schiff base derivatives containing heterocycles with aggregation-induced emission and recognition ability. J Mater Chem C 2014; 2: 2684−91;

(b) Kathiravan A, Sundaravel K, Jaccob M, Dhinagaran G, Rameshkumar A, Ananth DA, et al. Pyrene Schiff Base: Photophysics, Aggregation Induced Emission, and Antimicrobial Properties. J Phys Chem B 2014; 118: 13573−81;

(c) Tang WX, Xiang Y, Tong AJ. Salicylaldehyde azines as fluorophores of aggregation-induced emission enhancement characteristics. J Org Chem 2009; 74: 2163−6;

(d) Fang WY, Zhang GB, Chen J, Kong L, Yang LM, Bi H, et al. An AIE active probe for specific sensing of Hg^{2+} based on linear conjugated bis-Schiff base. Sens Actuators B 2016; 229: 338−46;

(e) Cheng JH, Li YX, Sun R, Liu J Y, Gou F, Zhou XG, et al. Functionalized salen ligands linking with non-conjugated bridges: unique and colorful aggregation-induced emission, mechanism, and applications. J Mater Chem C, 2015; 3: 11099−110.

[24] (a) Han T, Feng X, Chen D, Dong Y. A diethylaminophenol functionalized Schiff base: crystallization-induced emission-enhancement, switchable fluorescence and application for security printing and data storage. J Mater Chem C 2015; 3: 7446−54;

(b) Dong YQ, Lam JWY, Tang BZ. Mechanochromic luminescence of aggregation-induced emission luminogens. J Phys Chem Lett 2015; 6: 3429−36.

[25] (a) Roberts DRT, Holder SJ. Mechanochromic systems for the detection of stress, strain and deformation in polymeric materials. J Mater Chem 2011; 21: 8256−68;

(b) Mukherjee S, Thilagar P. Stimuli and shape responsive 'boron-containing' luminescent organic materials. J Mater Chem C 2016; 4: 2647−62;

(c) Xu F, Nishida T, Shinohara K, Peng L, Takezaki M, Kamada T, et al. Trimethylsilyl group assisted stimuli response: self-assembly of 1,3,6,8-tetrakis((trimethysilyl)ethynyl)pyrene. Organometallics 2017; 36: 556−63.

[26] (a) Stuart MAC, Huck WTS, Genzer J, Muller M, Ober C, Stamm M, et al. Emerging applications of stimuli-responsive polymer materials. Nat Mater 2010; 9: 101−13;

(b) Akita, M. Photochromic organometallics, a stimuli-responsive system: an approach to smart chemical systems. Organometallics 2011; 30: 43−51.

[27] Han F, Zhang R, Zhang Z, Su J and Ni Z. A new TICT and AIE-active tetraphenylethene-based Schiff base with reversible piezofluorochromism. RSC Adv 2016; 6: 68178−84.

[28] Jia JH, Wu Y. Synthesis, crystal structure and reversible mechanofluorochromic properties of a novel phenothiazine derivative. Dyes Pigm. 2017; 136: 657–62.

[29] Yang JS, Liau KL, Wang CM, Hwang CY. Substituent-dependent photoinduced intramolecular charge transfer in N-Aryl-substituted trans-4-aminostilbenes. J Am Chem Soc 2004; 126: 12325–35.

[30] Jones G, Jackson WR, Choi C, Bergmark WR. Solvent effects on emission yield and lifetime for coumarin laser dyes. Requirements for a rotatory decay mechanism. J Phys Chem 1985; 89: 294–300.

[31] Zhang Z, Zhang H, Jiao C, Ye K, Zhang H, Zhang J, et al. 2-(2-hydroxyphenyl)benzimidazole-hased four-coordinate boron-containing materials with highly efficient deep-blue photoluminescence and electroluminescence. Inorg Chem 2015; 54: 2652−9.

[32] Frisch MJ, Trucks GW, Schlegel HB, Scuseria GE, Robb MA, Cheeseman JR, Scalmani G, Barone V, Mennucci B, Petersson GA, Nakatsuji H, Caricato M, Li X, Hratchian HP, Izmaylov AF, Bloino J, Zheng G, Sonnenberg JL, Hada M, Ehara M, Toyota K, Fukuda R, Hasegawa J, Ishida M, Nakajima T, Honda Y, Kitao O, Nakai H, Vreven T, JA Montgomery, Peralta JE, Ogliaro F, Bearpark M, Heyd JJ, Brothers E, Kudin KN, Staroverov VN, Kobayashi R, Normand J, Raghavachari K, Rendell A, Burant JC, Iyengar SS, Tomasi J, Cossi M, Rega N, Millam JM, Klene M, Knox JE, Cross JB, Bakken V, Adamo C, Jaramillo J, Gomperts R, Stratmann RE, Yazyev O, Austin AJ, Cammi R, Pomelli C, Ochterski JW, Martin RL, Morokuma K, Zakrzewski VG, Voth GA, Salvador P, Dannenberg JJ, Dapprich S, Daniels AD, Farkas O, Foresman JB, Ortiz JV, Cioslowski J and Fox DJ, Gaussian 09, Revision A.01, Gaussian, Inc., Wallingford CT, 2009.

[33] (a) Hu LY, Duan YA, Xu ZZ, Yuan J, Dong YP, Han TY. Stimuli-responsive fluorophores with aggregation-induced emission: implication for dual-channel optical data storage. J Mater Chem C 2016; 4: 5334–41;

(b) Weil T, Vosch T, Hofkens J, Peneva K, Muellen K. The rylene colorant family–tailored nanoemitters for photonics research and applications. Angew Chem Int Ed 2010; 49: 9068–93;

(c) Sun J, Han J, LiuY, Duan Y, Han T, Yuan J. Mechanochromic luminogen with aggregation induced emission: implications for ink-free rewritable paper with high fatigue resistance and low toxicity. J Mater Chem C 2016; 4: 8276–83.

[34] Zhang X, Chi Z, Xu B, Chen C, Zhou X, Zhang Y, et al. End-group effects of piezofluorochromic aggregation-induced enhanced emission compounds containing distyrylanthracene. J Mater Chem 2012; 22: 18505–13.

[35] (a) Yang Z, Chi Z, Xu B, Li H, Zhang X, Li X, et al. High-Tg carbazole derivatives as a new class of aggregation-induced emission enhancement materials. J Mater Chem 2010; 20: 7352–9;

(b) Li H, Chi Z, Xu B, Zhang X, Yang Z, Li X, et al. New aggregation-induced emission enhancement materials combined triarylamine and dicarbazolyl triphenylethylene moieties. J Mater Chem 2010; 20: 6103–10;

(c) Zhang X, Chi Z, Xu B, Li H, Yang Z, Li X, et al. Synthesis of blue light emitting bis(triphenylethylene) derivatives: A case of aggregation-induced emission enhancement. Dyes Pigm 2011; 89: 56–62.

[36] (a) Zhang X, Yang Z, Chi Z, Chen M, Xu B, Wang C, et al. A multi-sensing fluorescent compound derived from cyanoacrylic acid. J Mater Chem 2010; 20: 292–8;

(b) Bloor D, Kagawa Y, Szablewski M, Ravi M, Clark SJ, Cross GH, et al. Matrix dependence of light emission from TCNQ adducts. J Mater Chem 2001; 11: 3053–62;

(c) Barbara PF, Rand SD, Rentzepis PM.Direct measurements of tetraphenylethylene torsional motion by picosecond spectroscopy. J Am Chem Soc 1981; 103: 2156–62.

[37] Dong S, Li Z, Qin J. New carbazole-based fluorophores: synthesis, characterization, and aggregation-induced emission enhancement. J Phys Chem B; 2009: 113, 434–41.

[38] Zhang P, Liu W, Niu G, Xiao H, Wang M, Ge J, et al. Coumarin-Based Boron Complexes with Aggregation-Induced Emission. J Org Chem 2017; 82: 3456−62.

Highlights

TPE-ND and **TPE-NDB** showed obvious AIE properties.

TPE-NDB possesses distinct mechanofluorochromism with large spectral shift of 97 nm.

TPE-NDB fluorescence color can be reversibly switched by the grinding-fuming processes.